Dalton Transactions

Accepted Manuscript

ROYAL SOCIETY OF CHEMISTRY

www.rsc.org/dalton

Dalton Transactions

RSCPublishing

ARTICLE

Structure, Magnetism and EPR Spectra of a (μ−Thiophenolato) (μ−Pyrazolato−*N,N′*) Double Bridged Dicopper(II) Complex

Cite this: DOI: 10.1039/x0xx00000x

Received 00th January 2014,
Accepted 00th January 2014

DOI: 10.1039/x0xx00000x

www.rsc.org/

Narjes Khadir,[a] Davar M. Boghaei,*[a] Abdeljalil Assoud,[b] Otaciro R. Nascimento,[c] Amanda Nicotina,[d] Luis Ghivelder,[d] Rafael Calvo,*[e]

A new binuclear copper(II) complex, namely $[Cu_2L(pz)(DMSO)]$, where L = 2,6−bis[(2−phenoxy)iminomethyl]−4−methylthiophenolate(3−) and pz = pyrazolate ligand, has been synthesized by a one−pot synthesis involving copper(II) acetate monohydrate, the S−protected ligand precursor 2−(*N,N*−dimethylthiocarbamato)−5−methylisophthalaldehyde di−2′−hydroxy anil, (I), and pyrazole, in which a metal−promoted S−deprotection reaction occurs during the formation of the complex. This was characterized by routine physicochemical studies, single crystal X−ray diffraction and electron paramagnetic resonance (EPR) techniques. The structure analysis reveals that there are copper centres in two different environments, a slightly distorted square planar and a distorted square−pyramidal, arranged in binuclear units. The EPR study of these binuclear units performed at 9.4 GHz in the temperature range between 4 and 293 K shows an antiferromagnetic interaction between Cu^{II} ions, and allows evaluating g factors g_x = 2.068(1), g_y = 2.091(1) and g_z = 2.165(1), with $\langle g \rangle$ = 2.108(1), an exchange coupling parameter $J_0 = -26(1)$ cm^{-1} (defined as $\mathcal{H}_{ex} = -J_0 \boldsymbol{S_1 \cdot S_2}$), and a zero field splitting of the ground triplet state described by $D = 86(2)\times10^{-4}$ cm^{-1} and $E = -48(3)\times10^{-4}$ cm^{-1}. These results are discussed and compared with existing literature.

Introduction

The design and synthesis of bimetallic compounds received much attention[1] because of their interesting physicochemical properties[2–4] and their relevance as synthetic models of certain polymetallic coordinated proteins.[5–7] Binuclear complexes of ions with unpaired spins also provided the basis of the field of molecular magnetism and have offered through the years a tantamount of new knowledge in physics and chemistry.[8–12] Indeed, the expectation that the two neighbouring metal centres should be able to interact magnetically and/or electrically, has led the preparation of bimetallic compounds to be an area of great current research interest to inorganic chemists.[13] An appropriate approach to constructing binuclear systems containing two metal centres in close proximity is the introduction of particular classes of binucleating "compartmental" ligands, i.e. "ligands whose bridging groups can contiguously accommodate two metals".[1,2] Along this line, in order to understand the factors responsible for the magnetic−exchange interactions occurring between metal centres coupled via bridging ligands, several types of binuclear metal complexes of compartmental ligands with various bridging groups such as pyrazolate,[14,15] phenolate,[16] alkoxide,[17] and thiophenolate[18] have been synthesized and studied structurally and magnetically.[19] While the peculiar magnetic properties of bimetallic complexes of phenol−based compartmental ligands have been widely investigated,[20–23] rather few papers have analyzed the magnetic properties of the corresponding thiophenolato−bridged complexes,[18,24,25] possibly because thiolates are more readily oxidized and the chemistry required to generate such compounds is less well−developed. Robson and co−workers[18,26] initially designed and synthesized two S−protected binucleating ligand precursors I and II (Scheme 1) from which some binuclear transition metal(II)−complexes were isolated (III in Scheme 1).[26–29] The free thiophenolato ligands are liberated via a metal−promoted S−deprotection process, occurring during the formation of the complex in a "one−pot" reaction. An additional bridging ligand Z may donate one (OR^-, Cl^-, etc.) or two (pyrazolate, acetate, etc.) atoms to the coordination spheres of the metals to the complexes of type III. After the pioneering work of

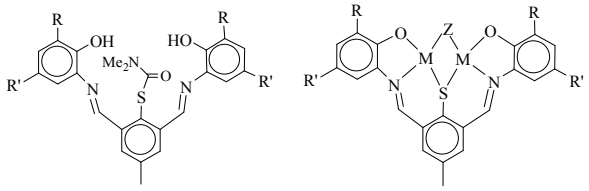

I R=R'=H
II R=R'=*tert*-butyl

III

Scheme 1 Molecular structure of ligands I and II and complex III; M = Ni^{2+}, Cu^{2+} and Pd^{2+}

Robson *et al*[18,26]. on these complexes, no research was found about this class of compartmental thiophenolato−bridged complexes, and according to the Cambridge structural database (CSD), no structural data are yet available for complexes type III.

In this work we report the preparation, crystal structure and magnetic properties of the new binuclear copper(II) complex, ((μ_2−2,6−bis((2−phenoxy)iminomethyl)−4−methylthiophenolato)−dimethyl sulfoxide−(μ_2−pyrazolato−*N,N'*)−di−copper(II), named [Cu_2L(pz)(DMSO)] where L = 2,6−bis[(2−phenoxy)iminomethyl]−4−methylthiophenolate(3−). To the best of our knowledge, this is the first crystallographically characterized transition metal complex of the di−Schiff−base binucleating ligand derived formally from the condensation of two equivalents of *o*−aminophenol with one equivalent of S−(2,6−diformyl−4−methylphenyl)dimethylthiocarbamate. A detailed electron paramagnetic resonance (EPR) study of powder samples in the temperature (*T*) range between 4 and 293 K was performed. Global fitting of a spin Hamiltonian[30] to these EPR spectra allows evaluating the anisotropic *g*−factors, the isotropic exchange interaction coupling J_0 (defined as[11] $\mathcal{H}_{ex} = -J_0\, \boldsymbol{S_1}\cdot\boldsymbol{S_2}$, where $\boldsymbol{S_1}$ and $\boldsymbol{S_2}$ are the interacting copper spins with $S = ½$), and the anisotropic spin−spin interaction parameters *D* and *E*.[31–34]

Experimental Section

Materials. All chemicals were obtained from commercial sources and used as received. Solvents were dried according to standard procedures and distilled prior to use. 2−(*N,N*−dimethylthiocarbamato)−5−methylisophthalaldehyde di−2'−hydroxy anil, (I), was prepared according to the literature method.[26] *o*−aminophenol was purchased from Aldrich Chemical Company, Inc.

Physical Measurements. Elemental analyses were performed on a Fison equipment model EA 1108. UV–Vis spectra were recorded with a CARY 100 Bio VARIAN UV–Vis spectrophotometer. Infrared spectra (4000–400 cm^{-1}) of solid samples were taken in KBr pellets using a Unicam Matson 1000 FT−IR Spectrophotometer.

Synthesis and Characterization of [Cu_2L(pz)(DMSO)]. A solution of the S−protected ligand precursor, I, (0.20 g, 0.47 mmol) and pyrazole (0.035 g, 0.55 mmol) in acetonitrile (CH_3CN, 40 cm^3) at 90°C were added to a hot solution of copper(II) acetate monohydrate (0.20 g, 0.98 mmol) in 15 cm^3 of DMSO. The intense brown solution was filtered and then allowed to stand at room temperature for three days. Crystals of [Cu_2L(pz)(DMSO)] suitable for X−ray data collection and to be ground for EPR measurements, were collected by filtration, washed with acetonitrile and dried at 80°C under vacuum. Yield, 0.1 g (33%). Anal. Calcd. for $C_{26}H_{24}N_4O_3S_2Cu_2$: C, 49.43; H, 3.83; N, 8.87; S, 10.15. Found: C, 48.83; H, 3.57; N, 8.23; S, 9.87. IR (KBr disk, cm^{-1}): 1644 (pyrazolate C=N st.), 1583 (imine C=N st.), 530 (Cu−O st.), 482 (Cu−N st.). UV−vis (DMF), [λ_{max}, nm (ε, $M^{-1}cm^{-1}$)]: 600 (sh), 478 (7210), 414 (7408), 319 (11801), 287 (10654).

X−ray Crystallography. Diffraction data were collected on a Bruker Kappa APEX II diffractometer using graphite−monochromated Mo−K_α radiation (λ= 0.71073 Å). Data were collected using ω− and ϕ− scans of 0.3° in groups of frames at different ω and ϕ with exposure times of 30 seconds per frame. They were corrected for Lorentz and polarization effects using the Bruker SAINT software package.[35] Absorption corrections were based on fitting a function to the empirical transmission surface as sampled by multiple equivalent measurements using SADABS.[36] The systematic absences indicate the monoclinic space group $\boldsymbol{P}2_1/c$. The structure of $C_{26}H_{24}N_4O_3S_2Cu_2$ was solved using the direct method and least squares refined with the Bruker SHELXTL software package.[37] The final anisotropic full−matrix least−squares refinement on F^2 with 334 variables converged to R_1 = 4.43% and wR_2= 8.24%. All hydrogen atoms in geometrically idealized positions were refined using a rigid model with C−H = 0.93 − 1 Å and isotropic displacement parameters $U_{iso}(H) = 1.2\, U_{eq}(C) - 1.5\, U_{eq}(C)$. Crystal data and experimental details are summarised in Table 1. Selected distances and angles in the structure are given in Table 2 and hydrogen bonding and π−π stacking parameters are summarized in Table 3 and Table S1 of ESI†, respectively.

Table 1 Selected Crystallographic Data for [Cu_2L(pz)(DMSO)]

Empirical formula	$C_{26}H_{24}Cu_2N_4O_3S_2$
Formula weight	631.69
Temperature (K)	296
Wavelength (Å)	0.71073
Crystal system	Monoclinic
Space group	$\boldsymbol{P}2_1/c$
Crystal colour, shape	Red, needle
Crystal size, mm×mm×mm	0.01 × 0.03 × 0.49
a (Å)	6.9313 (2)
b (Å)	14.7303 (5)
c (Å)	24.8075 (7)
α (°)	90
β (°)	94.823 (2)
γ (°)	90
V (Å³)	2523.88 (13)
μ, mm^{-1}	1.888
D_{calc}, g/cm^3	1.6626(1)
Z	4
F(0 0 0)	1288
Theta range for data collection	3.7−26.0°
Index ranges	−8≤ h ≤8
	0≤ k ≤18
	0≤ l ≤30
Maximum and minimum transmission	0.9906 and 0.4581
Refinement method	Full−matrix least−squares on F^2
Goodness−of−fit on F^2	0.996
R_1 and wR_2 indices [I > 2σ(I)]	R_1=0.0443, wR_2=0.0824
R_1 and wR_2 indices (all data)	R_1=0.0906, wR_2=0.0938
Largest difference in peak and hole (e Å^{-3})	0.388 and −0.338

EPR Measurements. Spectra were collected at 49 values of temperature (*T*) in the range between 4 and 293 K, using a Bruker Elexsys E580 spectrometer working at 9.462 GHz, with a cavity having ~1 mT of 100 KHz magnetic field modulation. A paramagnetic Cr^{III}:MgO field and signal intensity marker (*g* = 1.9797) was located with the sample. The small sizes of the available [Cu_2L(pz)(DMSO)] crystals do not allow single crystal EPR measurements and the spectra were collected in powder samples made by grounding small crystals. The spectra were globally analysed using EasySpin,[38] a package of programs working under Matlab.[39]

Experimental Results and Analysis

Crystal Structure of [Cu_2L(pz)(DMSO)]

Figure 1 displays the structure of the binuclear Cu^{II} molecular complex [Cu_2L(pz)(DMSO)], together with the atom labelling scheme. The asymmetric unit cell contains two crystallographically

independent Cu^{II} ions, Cu1 and Cu2, bonded to one pentadentate trianionic Schiff base ligand 2,6−bis[(2− phenoxy)iminomethyl]−4−methylthiophenolate(3−)*(L)* and one pyrazolate ion to form the binuclear complex. The Cu2 ion is also bound to a DMSO molecule. The Cu1 ion exhibits an approximate square planar coordination geometry with the value τ_4= 360°−(α+β)/141° = 0.1178(16), where α and β are the two largest angles in the four−coordinate species;[40] τ_4 would range from 1.00 for a perfect tetrahedral geometry to zero for a perfect square planar geometry. The Cu1 ion deviates 0.0264(14) Å from the least−squares plane through the four coordination centres. The geometry around the Cu2 ion is distorted square−pyramidal with the parameter τ_5= (β−α)/60°= 0.362(1) , with α and β being the two largest coordination angles; τ_5 would range from 1.00 for a perfect trigonal bipyramidal geometry to zero for a perfect square pyramidal geometry.[41] The basal planes for both, Cu1 and Cu2, consist of one μ−thiophenolate S−atom, one imine N−atom, and one phenoxo O−atom of the end−off compartmental ligand system and one N−atom of the bridging pyrazolate moiety. The apical position of the square pyramidal geometry around Cu2 is occupied by the oxygen atom of a DMSO molecule. The Cu2 atom is displaced 0.2067(13) Å towards the apical oxygen and, as it would be expected for a square pyramidal copper coordination, the apical distance Cu2–O3 = 2.375(3) Å is longer than the Cu−O bond length in the base [Cu2–O2 = 1.942(3) Å] due to the $\sigma^*(d_z^2)^2\sigma^*(d_{x^2-y^2})^1$ configuration of the copper(II) ion.[42] A search in CCDC on structurally characterized binuclear copper(II) complexes bridged on one side by an endogenous thiophenolate bridging ligand and on the other side by an exogenous pyrazolate bridging group, retrieved only one structure $[Cu_2(L-S)(pz)(CH_3OH)]$[18] possessing side groups attached to the thiophenolate ring different from those associated with our complex $[Cu_2L(pz)(DMSO)]$. In $[Cu_2L(pz)(DMSO)]$ and $[Cu_2(L-S)(pz)(CH_3OH)]$ the bridging thiophenolate−sulfur atom has approximately the same pyramidal configuration and the molecules are folded around the C−S axis. However, the dihedral angle of 3.85(12)° between adjacent N,N,O coordination planes in $[Cu_2L(pz)(DMSO)]$ is significantly smaller than the 16.0° observed in $[Cu_2(L-S)(pz)(CH_3OH)]$. Also, the Cu···Cu distance of 3.5926(3) Å and Cu−S−Cu angle of 108.32 (5)° are longer and greater than the values 3.474(3) Å and 101.5(2)° in $[Cu_2(L-S)(pz)(CH_3OH)]$. These differences may be a consequence of the fact that the pentadentate compartmental Schiff base ligand in $[Cu_2(L-S)(pz)(CH_3OH)]$ is more flexible than that in $[Cu_2L(pz)(DMSO)]$. As shown in Fig. 2, two adjacent centrosymmetrically related molecules of the complex along the *a*−axis are linked by a combination of weak N−H···O,

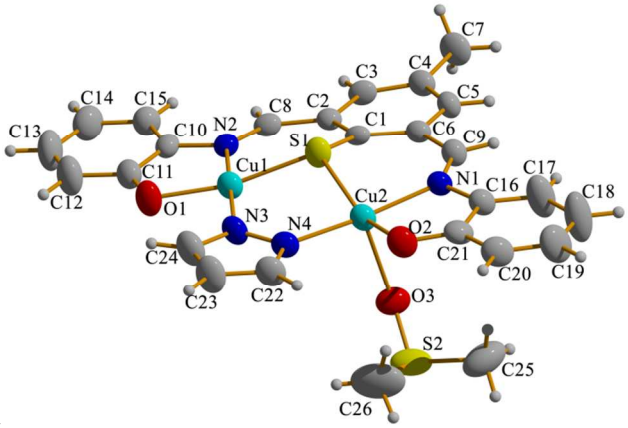

Fig. 1 Molecular structure of $[Cu_2L(pz)(DMSO)]$, showing the atom−labelling system and 50% thermal ellipsoids.

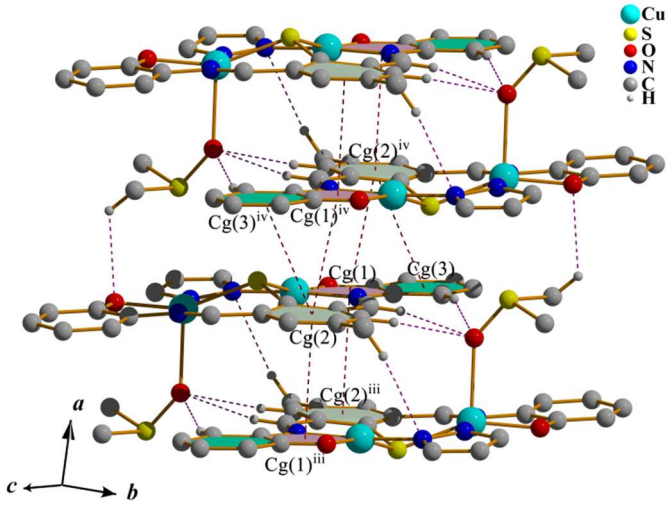

Fig. 2 Perspective view of the formation of a 1D chain due to non−classical hydrogen bond and weak π–π stacking interactions along the a−axis direction. Hydrogen atoms, except those involved in hydrogen−bonding interactions, are omitted for clarity.

trifurcated C−H···O and π–π stacking (Cg(1)→Cg(2)^{iii} and Cg(1)^{iii} → Cg(2)) interactions. Each of the units can be viewed as a tetramer having an inversion centre. These tetrameric units are nailed to two other tetramers on their adjacent sides by two symmetry−related C−H···O hydrogen bonds (Table 3) and two sets of π –π stacking interactions (Cg(2)^{iv} → Cg(1) and Cg(3), and Cg(2) → Cg(1)^{iv} and Cg(3)^{iv}) (Table S1 of ESI†). These interactions propagate, leading to the formation of 1D chains along the *a*−axis. These chains, in turn, self−assemble via electrostatic and van der Waals interactions to construct a three−dimensional network. The D···A distances of the C– H···O and C–H···N hydrogen bonds (see Table 3) range from 3.2537(65) to 3.6829(58) Å with H···O and H···N separations in the 2.4880(27)– 2.7781(27) Å range, distances falling into the range of distances previously reported for the C– H···O and C–H···N hydrogen bonds. [43,44]

Table 2 Selected distances and angles in the structure (Å, °)

Cu1-O1	1.899 (3)	Cu2-O2	1.942 (3)
Cu1-N3	1.954 (3)	Cu2-N4	1.971 (3)
Cu1-S1	2.2012 (12)	Cu2-S1	2.2301 (12)
Cu1-N2	1.973 (3)	Cu2-N1	1.991(3)
		Cu2–O3	2.375(3)
O1-Cu1-S1	167.27(10)	N4-Cu2-N1	175.42(13)
N2-Cu1-N3	176.11(13)	S1-Cu2-O2	153.70(9)
Cu1-S1-Cu2	108.32 (5)	C1-S1-Cu2	112.98 (13)
C1-S1-Cu1	113.23 (14)		

Table 3 Hydrogen−bond geometry (Å, °)

D—H···A	D—H	H···A	D···A	D—H···A
C3—H3A···O3i	0.93	2.5270(28)	3.3936(51)	155.44
C8—H8A···O3i	0.93	2.4880(27)	3.3735(47)	159.46
C15—H15A···O3i	0.93	2.7781(27)	3.6756(49)	162.63
C7—H7C···N3i	0.96	2.7699(33)	3.6829(58)	159.07
C25ii—H25Bii···O2	0.96	2.6067(28)	3.2537(65)	124.96

Symmetry codes: (i) = 6−x, 2−y, −z; (ii) = x+1, y, z.

Electronic Spectra

The electronic spectrum of the complex $[Cu_2L(pz)(DMSO)]$ recorded in DMF solution is shown in Fig. S1 of ESI.† The binuclear complex exhibits a broad d−d absorption band at 591 nm in the form of a shoulder, as expected for a Cu(II) centre in an essentially planar four−coordinate coordination sphere or five−coordinate pyramidal geometry.[17] The bands observed at 478 and 414 nm were ascribed to the $PhO^-\rightarrow$Cu(II) and $PhS^-\rightarrow$Cu(II) transitions respectively.[45,46] A strong absorption around 319 nm is assigned to a Cu(II)→pyrazolate transition[47] and the strong band appearing below 300 nm is due to intraligand charge−transfer transition.[48]

EPR Results and Discussion

Figure 3 displays selected spectra collected at various temperatures. A microwave power of 2.5 mW producing no signal saturation of the sample or the marker within the studied T range was chosen to avoid saturation and obtain linear responses at any T, so the EPR signal intensities are proportional to the magnetic susceptibility.[49,50] Under these conditions the EPR measurements reported here provide spectroscopic information related to the shape of the spectra, and thermodynamic information related to the changes of intensity in the studied T range. The peak−to−peak signal intensity displays a maximum at $T \sim 24$ K and decreases at lower and higher T, as shown in Fig. 4; Fig. 5 displays the spectrum observed at 24 K. The behaviour displayed by the EPR results in Figs. 3−5 is that expected for an antiferromagnetically coupled binuclear copper compound with an exchange interaction parameter J_0 close in T units to the position of the intensity peak in Fig. 4. Even in the spectra of a powder sample, one should observe at low T traces of the classical seven−peaks pattern of the hyperfine structure for copper binuclear units.[8,30,51] The absence of this structure at any temperature may be attributed to the interactions between copper ions in neighbouring binuclear units.[33,34] At the lowest temperatures one observes an important contribution to the spectra of traces of paramagnetic mononuclear copper, present as impurities or lattice defects, with intensity following a Curie−Weiss law $1/T$ dependence, as occurs in most susceptibility measurements for antiferromagnetic units.[11]

The EPR data displayed in Figs. 3−5 is analysed with the spin Hamiltonian:

$$\mathcal{H}_0 = \mu_B \boldsymbol{B_0}\cdot(\boldsymbol{g_1}\cdot\boldsymbol{S_1}+\boldsymbol{g_2}\cdot\boldsymbol{S_2}) - J_0\,\boldsymbol{S_1}\cdot\boldsymbol{S_2} + \boldsymbol{S_1}\cdot\boldsymbol{D}\cdot\boldsymbol{S_2} \qquad (1)$$

The first term on the right side of eqn 1 is the Zeeman contribution of the spins $\boldsymbol{S_1}$ and $\boldsymbol{S_2}$ of the copper ions, the second is the intradinuclear isotropic exchange coupling between $\boldsymbol{S_1}$ and $\boldsymbol{S_2}$, and the third is the anisotropic spin−spin interaction between the spins, arising from dipole−dipole and anisotropic exchange. One of the consequences of the exchange J_0 is to average out the differences between $\boldsymbol{g_1}$ and $\boldsymbol{g_2}$ to $\boldsymbol{g} = (\boldsymbol{g_1} + \boldsymbol{g_2})/2$ in eqn 1.[52] Since measurements in powder samples do not allow evaluating their relative orientations, we assume that the average matrix $\boldsymbol{g}$ has the same principal axes as the spin−spin interaction matrix $\boldsymbol{D}$. In fact we used the spin Hamiltonian:

$$\mathcal{H}_S = \mu_B\,\boldsymbol{B_0}.\boldsymbol{g}.(\boldsymbol{S_1}+\boldsymbol{S_2}) - J_0\,\boldsymbol{S_1}.\boldsymbol{S_2} + D\,[S_{1z}S_{2z} - \boldsymbol{S_1}.\boldsymbol{S_2}/3] + E\,[S_{1x}S_{2x} - S_{1y}S_{2y}] \qquad (2)$$

where $\boldsymbol{g}$ is diagonal with principal values g_x, g_y and g_z. Fitting $\mathcal{H}_S$ to the observed spectra and their variation with T allows obtaining g_x, g_y and g_z, the exchange coupling J_0 and the principal values D and E of the traceless matrix $\boldsymbol{D}$. In fact, the most important source of uncertainty in the parameters of the fit arises from the line width ΔH

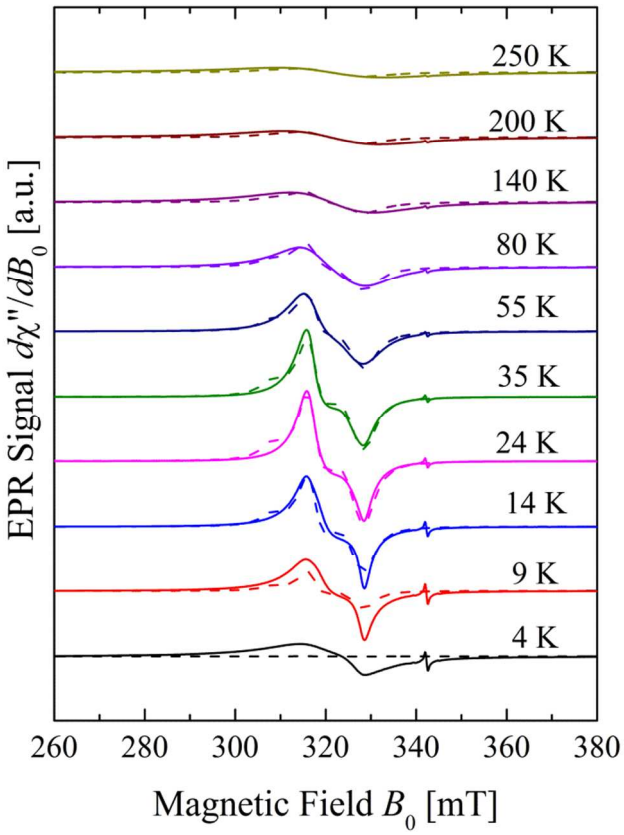

Fig. 3 EPR spectra of $[Cu_2L(pz)(DMSO)]$ obtained at selected temperatures. Solid lines are experimental results. Dotted lines are simulations obtained as described in the text.

assumed in the simulations, which in principle may be a function of field orientation and of T. To model that would add too many parameters to the fitting. So, we assumed isotropic ΔH, constant at low T but growing linearly with T above 40 K; the data indicate a Lorentzian line shape. Using EasySpin,[38] together with optimization programs provided by Matlab[39] we evaluated the parameters fitting eqn 2 to the data. The g−factors and D and E depend mainly of the shape of the spectra, while the exchange coupling J_0 is mainly determined by the temperature variation of the intensity of the spectrum. The most important spectra in this fitting (some of them shown in Fig. 3) are those having the largest intensity at T around the maximum at ~24 K shown by Fig. 4. The values of the parameters obtained from the fit are $g_x = 2.068(1)$, $g_y = 2.091(1)$ and $g_z = 2.165(1)$, with $\langle g \rangle = 2.108(1)$, $J_0 = -26(1)$ cm^{-1}, $D = \pm 86(2)\times10^{-4}$ cm^{-1} and $E = \mp 48(3)\times10^{-4}$ cm^{-1}, where the sign of J_0 indicates antiferromagnetic exchange and D and E have opposite signs. The isotropic width calculated from the fit is ΔH = 6.2 mT, increasing 0.03 mT/K above 40 K. Figures 3 and 4 show the results of the fittings that are in good agreement with the data in the important T range; the simulation of the spectrum at 24 K is shown in Fig. 5. Discrepancies between fittings and data observed below 10 K, are attributed to traces of paramagnetic impurities; differences between data and simulations, as those observed in Fig. 5 at fields B_0 = 305 mT and 320 mT, are attributed to an angular variation of the line width that cannot be simulated without overparameterization of the fits. In any case, we verified that these discrepancies do not hamper the result of the fitting.

There are six different ways to define the D and E parameters, which

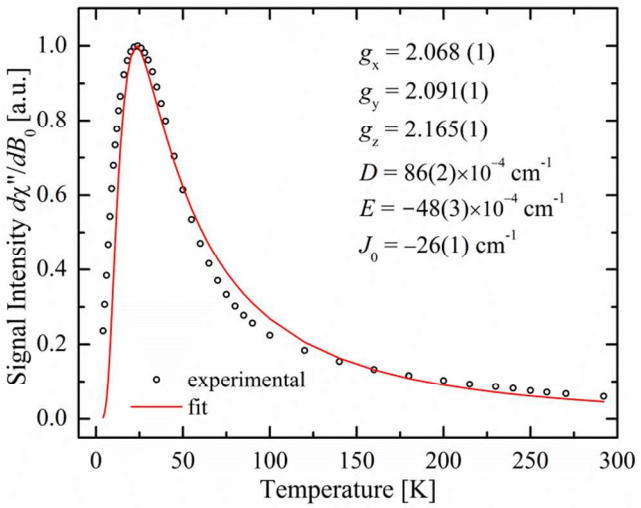

Fig. 4 Temperature variation of the full amplitude of the EPR signal $d\chi''/dB_0$. Circles are experimental values. The solid line is a simulation obtained with the given parameters.

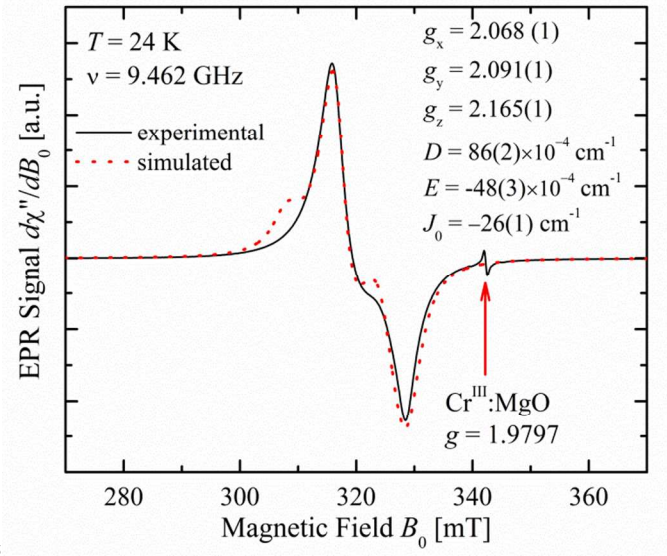

Fig. 5 EPR spectrum of $[Cu_2L(pz)(DMSO)]$ at $T = 24$ K. The solid line is the experimental result and the dotted line is a simulation obtained with the given parameters.

depend on the coordinate frame used for eqn 2. A standard rule chooses a frame where $|D| > 3|E|$.[30,53,54] However, the g-factor for Cu^{II} ions is anisotropic and our experiments allow to measure this anisotropy; so we chose as reference frame in eqn 2 the one resulting from the standard rule for anisotropic g-factors, $g_x < g_y < g_z$.

The $\boldsymbol{g}$-matrices for Cu^{II} ions are a consequence of the admixture of excited states into the ground orbital state $d_{x^2-y^2}$ due to the spin orbit interaction. This admixture increases the g-factor from the spin-only $g = 2.00232$, and the values normally observed in a square of N or O ligands are $g_\perp \sim 2.05$–2.07 in the equatorial plane and $g_{//} \sim 2.3$ along its normal. The presence of an S atom in the coordination plane may distort somewhat these values, but the change is not expected to be large. The rhombicity of the observed g-matrix results when passing from eqn 1 to eqn 2 considering that the exchange coupling J_0 averages out g_1 and g_2 for each field orientation.[55,56] The obtained average $\langle g \rangle = 2.108(1)$ is that expected for Cu^{II} ions. The zero field parameters D and E (eqn 2) split the triplet state and are the consequence of magnetic dipole–dipole interactions and anisotropic exchange. Only EPR experiments at high field and low T may provide their individual signs, our experiments only provide the relative signs.[57,58] Since the signal intensity of antiferromagnet dinuclear units decrease to zero at low T, the only way to obtain the signs is to perform experiments at microwave frequencies in the range of hundreds of gigahertz. Nevertheless, we compare the measured magnitudes with estimations of the dipole–dipole interaction assuming point dipolar behaviour, and the anisotropic exchange coupling considering the classic calculation of Moriya[59] and the results of Bencini and Gatteschi.[10] The point charge estimate of the dipolar interaction is[51] $D_{dip} \sim 3g^2\mu_B^2/(2R^3)$, where R is the distance between spins, in our case $R = 3.592$ Å. So, the estimated dipolar contribution is $D_{dip} \sim 0.07$ cm−1. On the other side, and according Moriya,[59] the anisotropic exchange contribution is $D_{anis} \approx (\Delta g/g)^2 J_0 \sim -0.14$ cm^{-1}, where Δg is the average deviation of the g factor from the spin only value 2.0023. Thus, since both contributions are larger than the measured value and of opposite sign, any conclusion regarding D is doubtful. In addition, Moriya's approximation[59] has been criticized as being not reliable.[10]

Correlation Between Structural and Magnetic Results

Superexchange is a quantum effect, so, when the path connecting the metal ions is composed of two independent chemical paths, their individual contributions do not sum but interfere, and this interference may be constructive or destructive.[11,60–62] Even minor changes in the individual paths may produce relevant changes in the magnitude of the exchange parameter J_0. This phenomenon, was described as orbital complementarity and counter-complementarity by Nishida and Kida.[63] The magnetic behaviour of $[Cu_2L(pz)(DMSO)]$, like other heterobridged complexes could be explained by a two-step perturbation process.[60–63] In the first step, in the absence of the pyrazolate ligand, the symmetric φ_S and antisymmetric φ_{AS} combinations of the magnetic orbitals are mixed in an antibonding way with the bridging sulfur p_y and p_x orbitals, respectively, to form new symmetric φ_S' and antisymmetric φ_{AS}' combinations, so that φ_{AS}' would be higher in energy due to substantially larger overlap integral resulting from the relatively large Cu–S–Cu bridging angle (107°).[11,63,64] In the second step, as predicted by Nishida and Kida,[63,65] antibonding interactions of φ_S' with the symmetric Homo of pyrazolate and φ_{AS}' with the antisymmetric Homo of pyrazolate result in new combinations of φ_S'' and φ_{AS}'', respectively. So it follows that the pyrazolate group exerts a complementarity effect.[16,63,66] The antiferromagnetic coupling is proportional to the energy difference $\Delta\varepsilon = \varepsilon(\varphi_{AS}'') - \varepsilon(\varphi_S'')$,[60] where the relative energies of φ_S'' and φ_{AS}'' depend on the energy differences and the overlap integrals between the interacting orbitals.[60]

constant

The effect of the energy factor on the exchange coupling constant was investigated by Vicente et al.,[67] who pointed out that the value of $|J_0|$ for the planar binuclear copper(II) compounds with bisbidentate bridging ligands significantly increase when oxalate ($J_0 = -384$ cm^{-1}) is replaced by tetrathiooxalato ($|J_0| > 800$ cm^{-1}). The enhancement of the interaction, compared to the oxalato-bridged compound can be understood in the light of a molecular orbital model: the sulfur 3s and 3p valence orbitals are higher in energy than the oxygen 2s and 2p orbitals and this results in a reduction of the energy gap between the HOMOs of tetrathiooxalato and the copper d orbitals, which favors a stronger metal-bridge interaction. So, stronger antiferromagnetic interactions would be expected when an oxygen bridging atom is replaced with a sulfur atom, provided that the magnetic orbitals remain localized in the plane of the bridging

network.[9]

The importance of the orbital−overlap factor was emphasized by a computational analysis of a series of $Cu_2Cl_6^{2-}$ compounds[60] having essentially the same level ordering of the two highest metal orbitals as the alkoxido−, phenolato− and thiophenolato−bridged series. In this study[60] it was established that as the bridging atom is lifted out of the molecular plane, the antibonding overlaps of φ_S with p_y and φ_{AS} with p_x decrease. This would in turn lead to decrease the energies of both, the symmetric ($\varphi_{S''}$) and antisymmetric ($\varphi_{AS''}$), orbitals but the energy decrease of $\varphi_{S''}$ is smaller than that of $\varphi_{AS''}$, because in the twisted geometry the symmetric combinations of the magnetic orbitals (φ_S) can also interact in an antibonding way with the p_z orbital of the bridging atom to compensate partially for this loss.[60] As a result, the energy gap between symmetric and antisymmetric orbitals ($\varepsilon(\varphi_{AS''})$–$\varepsilon(\varphi_{S''})$) is reduced, thus leading to a weaker antiferromagnetic interaction. As an example, due to the pyramidal disposition of the sulfur bridge atom, the antiferromagnetic interactions in thiophenolato/pyrazolato−bridged complexes is significantly weaker than the coupling observed for a related series of the approximately planar phenolato/pyrazolato− and alkoxido/pyrazolato−bridged complexes, $[Cu_2(L-O)(pz)]$, where L=2,6−bis(4'−cyclohexyl−4'−hydroxy−2',3'−diazabuta−1',3'−dien−1'−yl)−4−methyl−phenolate(3−) (J_0 = −382 cm^{-1}),[18] 2,6−bis[(2−phenoxy)iminomethyl]−4−methylphenolate(3−) (J_0 = −457 cm^{-1}),[16] 1,3−bis(salicylideneamino)propan−2−ol (J_0 = −310 cm^{-1}),[63] 1,4−bis(salicylideneamino)butan−2−ol (J_0 = −545.6 cm^{-1}),[68] and 1,5−bis(salicylideneamino)pentan−3−ol (J_0 = −595 cm^{-1}).[63] The antiferromagnetic coupling J_0 = −26(2) cm^{-1} obtained here for $[Cu_2L(pz)(DMSO)]$ is stronger than J_0 = −3.6 cm^{-1} (using our definition of J_0) reported for $[Cu_2(L-S)(pz)(CH_3OH)]$[18] due to the smaller displacement of the bridging sulfur atom from the Cu−ligand best−plane and the greater Cu−S−Cu angle in the former compound.

Conclusions

We synthesized and structurally characterized the new binuclear copper(II) complex $[Cu_2L(pz)(DMSO)]$. The crystal structure analysis reveals that the two copper ions are doubly bridged by a common exogenous pyrazolate group and an endogenous thiophenolate−sulfur atom with a Cu···Cu distance of 3.5926(3) Å. The EPR spectra measured as a function of *T* allowed to evaluate the anisotropic *g*−matrix, the isotropic exchange J_0, and the anisotropic contributions to the spin−spin couplings, *D* and *E*. EPR is not the most frequent application used to study magnetic properties, but it worked very well in our problem, where we analysed the response of a small sample (< 1 mg).[10,52] Susceptibility data generally provide only an average *g*−factor and J_0; EPR provides the anisotropy of *g*, and also *D* and *E*. The observed orthorhombic symmetry of the anisotropic *g*−matrix is a consequence of the merging of the individual *g*−factors, due to the exchange coupling. The value of the antiferromagnetic exchange coupling J_0 = −26 cm^{-1}, much larger than a value reported before for a similar system,[18] is analysed in terms of current theories. In recent papers we have shown that EPR allows measuring very small interactions between dinuclear units,[34] even when they are combined with much larger couplings. These measurements, however, would require single crystal samples that were not available in this work.

Acknowledgements

NK and DMB are grateful to the Research Council of Sharif University of Technology for their financial support. RC is a member of CONICET, Argentina and received support from CAI+D−UNL.

Notes and references

[a] *Department of Chemistry, Sharif University of Technology, P.O. Box 11155−3516, Tehran, Iran. E−mail: dboghaei@sharif.ir*
[b] *Department of Chemistry, University of Waterloo, Waterloo, Ontario N2L 3G1, Canada*
[c] *Grupo de Biofísica Molecular Sergio Mascarenhas, Departamento de Física e Ciência Interdisciplinar, Instituto de Física de São Carlos, Universidade de São Paulo, CP 369, 13560−970 São Carlos, SP, Brazil.d*
[d] *Instituto de Física, Universidade Federal do Rio de Janeiro, CP 68528, 21941−972, Rio de Janeiro RJ, Brazil.*
[e] *Departamento de Física, Facultad de Bioquímica y Ciencias Biológicas, Universidad Nacional del Litoral, and Instituto de Física del Litoral, CONICET−UNL. Güemes 3450, 3000 Santa Fe, Argentina. E−mail: calvo.rafael@conicet.gov.ar*

† Electronic Supplementary Information (ESI) available: CCDC reference number 1021600. For crystallographic data in CIF format see DOI: 10.1039/b000000x/ . ESI also includes Fig. S1 with the electronic spectra and Table S1 with π-π stacking interaction parameters.

1 A. L. Gavrilova and B. Bosnich, *Chem. Rev.*, 2004, **104**, 349–384.
2 P. Guerriero, S. Tamburini and P. A. Vigato, *Coord. Chem. Rev.*, 1995, **139**, 17–243.
3 D. Kong, J. Reibenspies, J. Mao, A. Clearfield and A. E. Martell, *Inorg. Chim. Acta*, 2003, **342**, 158–170.
4 U. Casellato, S. Tamburini, P. Tomasin and P. A. Vigato, *Inorg. Chim. Acta*, 2004, **357**, 4191–4207.
5 N. Kitajima, *Adv. Inorg. Chem*, 1992, **39**, 1–77.
6 J. M. Berg, J. L. Tymoczko and L. Stryer, *Biochemistry*, W. H. Freeman & Co., New York, 2001.
7 M. Jarenmark, H. Carlsson and E. Nordlander, *Comptes Rendus Chim.*, 2007, **10**, 433–462.
8 B. Bleaney and K. D. Bowers, *Proc. R. Soc. A*, 1952, **214**, 451–465.
9 O. Kahn, *Angew. Chem., Int. Ed. Engl.*, 1985, **24**, 834–850.
10 A. Bencini and D. Gatteschi, *Electron Paramagnetic Resonance of Exchange Coupled Systems*, Springer-Verlag, Berlin, 1990.
11 O. Kahn, *Molecular Magnetism*, Wiley VCH, New York, 1993.
12 O. Kahn, *Acc. Chem. Res.*, 2000, **33**, 647–657.
13 P. A. Vigato, V. Peruzzo and S. Tamburini, *Coord. Chem. Rev.*, 2012, **256**, 953–1114.
14 J. Klingele, S. Dechert and F. Meyer, *Coord. Chem. Rev.*, 2009, **253**, 2698–2741.
15 S. O. Malinkin, Y. S. Moroz, L. V. Penkova, V. V. Bon, E. Gumienna-Kontecka, V. A. Pavlenko, V. I. Pekhnyo, F. Meyer and I. O. Fritsky, *Polyhedron*, 2012, **37**, 77–84.
16 W. Mazurek, A. M. Bond, K. S. Murray, M. J. O'Connor and A. G. Wedd, *Inorg. Chem.*, 1985, **24**, 2484–2490.
17 W. Mazurek, K. J. Berry, K. S. Murray, M. J. O'Connor, M. R. Snow and A. G. Wedd, 1982, 3071–3080.
18 P. Iliopoulos, K. S. Murray, R. Robson, J. Wilson and G. A. Williams, *J. Chem. Soc., Dalton Trans.*, 1987, 1585–1591.

19 P. Chaudhuri, V. Kataev, B. Büchner, H.-H. Klauss, B. Kersting and F. Meyer, *Coord. Chem. Rev.*, 2009, **253**, 2261–2285.

20 J. W. Pyrz, K. D. Karlin, T. N. Sorrell, G. C. Vogel and L. Que, *Inorg. Chem.*, 1984, **23**, 4581–4584.

21 A. Asokan, B. Varghese and P. T. Manoharan, *Inorg. Chem.*, 1999, **38**, 4393–4399.

22 S. Mukherjee, T. Weyhermüller, E. Bothe, K. Wieghardt and P. Chaudhuri, *Eur. J. Inorg. Chem.*, 2003, 863–875.

23 H. Wang, L.-F. Zhang, Z.-H. Ni, W.-F. Zhong, L.-J. Tian and J. Jiang, *Cryst. Growth Des.*, 2010, **10**, 4231–4234.

24 J. Lach, S. V. Voitekhovich, V. Lozan, P. N. Gaponik, O. A. Ivashkevich, J. Lincke, D. Lässig and B. Kersting, *Zeitschrift für Anorg. und Allg. Chemie*, 2010, **636**, 1980–1986.

25 J. Hausmann, M. H. Klingele, V. Lozan, G. Steinfeld, D. Siebert, Y. Journaux, J. J. Girerd and B. Kersting, *Chem. Eur. J.*, 2004, **10**, 1716–28.

26 J. G. Hughes and R. Robson, *Inorg. Chim. Acta*, 1979, **36**, 237–242.

27 A. M. Bond, M. Haga, I. S. Creece, R. Robson and J. C. Wilson, *Inorg. Chem.*, 1988, **27**, 712–721.

28 B. F. Hoskins, R. Robson, G. A. Williams and J. C. Wilson, *Inorg. Chem.*, 1991, **30**, 4160–4166.

29 A. M. Bond, M.-A. Haga, I. S. Creece, R. Robson and J. C. Wilson, *Inorg. Chem.*, 1989, **28**, 559–566.

30 J. A. Weil and J. R. Bolton, *Electron Paramagnetic Resonance. Elementary Theory and Practical Applications*, Wiley-Interscience, Hoboken, New Jersey, 2nd edn., 2007.

31 J. R. Wasson, C.-I. Shyr and C. Trapp, *Inorg. Chem.*, 1968, **7**, 469–473.

32 L. M. B. Napolitano, O. R. Nascimento, S. Cabaleiro, J. Castro and R. Calvo, *Phys. Rev. B*, 2008, **77**, 214423.

33 M. Perec, R. Baggio, R. P. Sartoris, R. C. Santana, O. Peña and R. Calvo, *Inorg. Chem.*, 2010, **49**, 695–703.

34 R. Calvo, J. E. Abud, R. P. Sartoris and R. C. Santana, *Phys. Rev. B*, 2011, **84**, 104433.

35 *Bruker Saint Plus Data Reduction and Correction Program, V. 6.01, Bruker AXS, Madison Wisconsin, USA*, Madison, Wisconsin, USA, 1998.

36 G. M. Sheldrick, *SADABS Siemens Area Detector Absorption Correction Program, v. 2.01*, Bruker/Siemens, Madison, Wisconsin, USA, 1998.

37 G. M. Sheldrick, *SHELXTL. Structure determination software suite, v.5.1. Bruker, Madison, Wisconsin, USA*, Madison, Wisconsin, USA, 1998.

38 S. Stoll and A. Schweiger, *J. Magn. Reson.*, 2006, **178**, 42–55.

39 Matlab, *The Mathworks Inc.*, Natick, MA 01760, 2012.

40 L. Yang, D. R. Powell and R. P. Houser, *Dalton Trans.*, 2007, 955–964.

41 A. W. Addison, T. N. Rao, J. Reedijk, J. van Rijn and G. C. Verschoor, *J. Chem. Soc., Dalton Trans.*, 1984, 1349–1356.

42 S. Balboa, R. Carballo, A. Castiñeiras, J. M. González-Pérez and J. Niclós-Gutiérrez, *Polyhedron*, 2008, **27**, 2921–2930.

43 F. A. Cotton, L. M. Daniels, G.T. Jordan IV and C. A. Murillo, *Chem. Commun.*, 1997, 1673–1674.

44 C. Janiak and T. G. Scharmann, *Polyhedron*, 2003, **22**, 1123–1133.

45 N. Aoi, G. Matsubayashi and T. Tanaka, *J. Chem. Soc., Dalton Trans.*, 1987, 241–247.

46 S. Anbu, M. Kandaswamy, P. Suthakaran, V. Murugan and B. Varghese, *J. Inorg. Biochem.*, 2009, **103**, 401–10.

47 J. Ackermann, F. Meyer, E. Kaifer and H. Pritzkow, *Chem. Eur. J.*, 2002, 247–258.

48 S. Mukhopadhyay, D. Mandal, P. B. Chatterjee, C. Desplanches, J.-P. Sutter, R. J. Butcher and M. Chaudhury, *Inorg. Chem.*, 2004, **43**, 8501–8509.

49 R. Kubo and K. Tomita, *J. Phys. Soc. Japan*, 1954, **9**, 888–919.

50 G. E. Pake, *Paramagnetic Resonance. An Introductory Monograph*, W. A. Benjamin, New York, 1962.

51 A. Abragam and B. Bleaney, *Electron Paramagnetic Resonance of Transition Ions*, Clarendon Press, Oxford, 1970.

52 R. Calvo, *Appl. Magn. Reson.*, 2007, **31**, 271–299.

53 P. L. Hall, B. R. Angel and J. P. E. Jones, *J. Magn. Reson.*, 1974, **15**, 64–68.

54 R. Kripal, D. Yadav, P. Gnutek and C. Rudowicz, *J. Phys. Chem. Solids*, 2009, **70**, 827–833.

55 R. Calvo, M. A. Mesa, G. Oliva, J. Zukerman-Schpector, O. R. Nascimento, M. Tovar and R. Arce, *J. Chem. Phys.*, 1984, **81**, 4584–4591.

56 N. M. C. Casado, R. A. Isaacson and R. Calvo, *J. Inorg. Biochem.*, 2001, **84**, 201–206.

57 R. Calvo, R. A. Isaacson, M. L. Paddock, E. C. Abresch, M. Y. Okamura, A.-L. Maniero, L. C. Brunel and G. Feher, *J. Phys. Chem. B*, 2001, **105**, 4053–4057.

58 A. Ozarowski, *Inorg. Chem.*, 2008, **47**, 9760–9762.

59 T. Moriya, *Phys. Rev.*, 1960, **120**, 91–97.

60 P. J. Hay, J. C. Thibeault and R. Hoffmann, *J. Am. Chem. Soc.*, 1975, **97**, 4884–4899.

61 P. R. Levstein, H. M. Pastawski and J. L. D'Amato, *J. Phys. Condens. Matter*, 1990, **2**, 1781–1794.

62 J. Curély and B. Barbara, *Struct. Bond*, 2006, **122**, 207–250.

63 Y. Nishida and S. Kida, *Inorg. Chem.*, 1988, **27**, 447–452.

64 A. Bencini and D. Gatteschi, *Inorg. Chim. Acta*, 1978, **31**, 11–18.

65 E. Spodine, A. M. Atria, J. Manzur, A. M. García, M. T. Garland, A. Hocquet, E. Sanhueza, R. Baggio, O. Peña and J.-Y. Saillard, *J. Chem. Soc., Dalton Trans.*, 1997, 3683–3689.

66 H. Nie, S. M. J. Aubin, M. S. Mashuta, R. A. Porter, J. F. Richardson, D. N. Hendrickson and R. M. Buchanan, *Inorg. Chem.*, 1996, **35**, 3325–3334.

67 R. Vicente, J. Ribas, S. Alvarez, A. Segui, X. Solans and M. Verdaguer, *Inorg. Chem.*, 1987, **26**, 4004–4009.

68 T. N. Doman, D. E. Williams, J. F. Banks, R. M. Buchanan, H.--R. Chang, R. J. Webb and D. N. Hendrickson, *Inorg. Chem.*, 1990, **29**, 1058–1062.

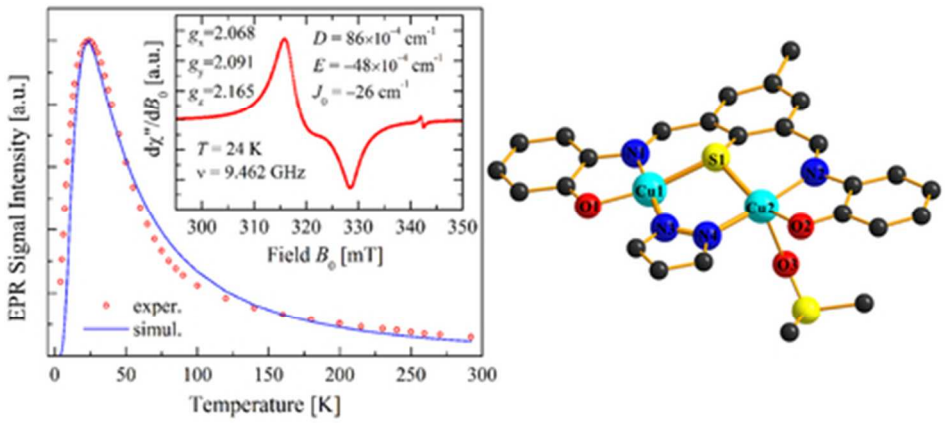

The structure and EPR spectra of the new compound [Cu_2L(pz)(DMSO)] are reported
39x17mm (300 x 300 DPI)